New Zealand Journal of Geology and Geophysics, 1999, Vol. 42: 155–168
0028–8306/99/4202–0155 $7.00/0

Geology, petrology, and petrogenesis of Little Barrier Island, Hauraki Gulf, New Zealand

JAN M. LINDSAY*
TIM J. WORTHINGTON
IAN E. M. SMITH
PHILIPPA M. BLACK
Department of Geology
The University of Auckland
Private Bag 92019
Auckland, New Zealand

*Present address: GeoForschungsZentrum Potsdam, P.B. 4.2, 14473 Potsdam, Germany.

Abstract Little Barrier Island is the emergent part of a large, isolated, dacite–rhyodacite volcano in the active Hauraki Rift, 80 km northeast of Auckland. Two volcanic episodes are recognised: Waimaomao Formation was emplaced as a rhyodacite dome at 3 Ma, whereas the more extensive dacitic lavas of Haowhenua Formation were erupted between 1.2 and 1.6 Ma. All Little Barrier lavas are strongly porphyritic and contain phenocrysts of plagioclase, orthopyroxene, and hornblende. Geochemically, they are subduction related and distinct from the older lavas of the Coromandel Volcanic Group, being Zr rich but Rb and Ba poor. Their Sr and Nd isotope ratios are similar to those of the Tonga–Kermadec arc volcanoes. Modelling of the dacite supports petrographic evidence that recharge and mixing were important in the magmatic system. Little Barrier and two dacite domes of similar age and composition near Whangarei form a northwest-trending lineament subparallel to the Alexandra Volcanics and the Vening Meinesz Fracture Zone.

Keywords volcano; dacite; K-Ar; geochemistry; Little Barrier Island; Hauraki Rift

INTRODUCTION

The northern part of the North Island of New Zealand is characterised by a complex succession of late Tertiary–Recent volcanic rocks. Along and to the west of the Northland Peninsula are the predominantly submarine complexes of the early Miocene Waitakere Arc (Hayward 1993). Deeply eroded volcanic centres of mid-Miocene to early Pliocene age crop out along the Coromandel Peninsula (Adams et al. 1994), and Pleistocene–Recent volcanism occurs throughout the Taupo Volcanic Zone (Wilson et al. 1995). In addition, several volcanic fields of mid-Miocene–Recent intraplate basalt occur between Kawhia and Kaikohe, including the young cones of the Auckland Volcanic Field (Smith 1989).

Little Barrier Island, located in the Hauraki Gulf at latitude 36°12′S, longitude 175°07′E, is a prominent feature of the skyline northeast of Auckland (Fig. 1). It has long been recognised as a volcano, and has a relatively uneroded conical form. Nevertheless, its geology has been the subject of only three significant studies (Hamilton 1937; Hopgood & Barron 1954; Kear 1961). From these, the volcano was thought to be of mid-Pleistocene age and its lavas andesitic.

Here, we examine the volcanic history and petrologic evolution of Little Barrier volcano using new K-Ar and U-Pb age determinations for selected samples and geochemical

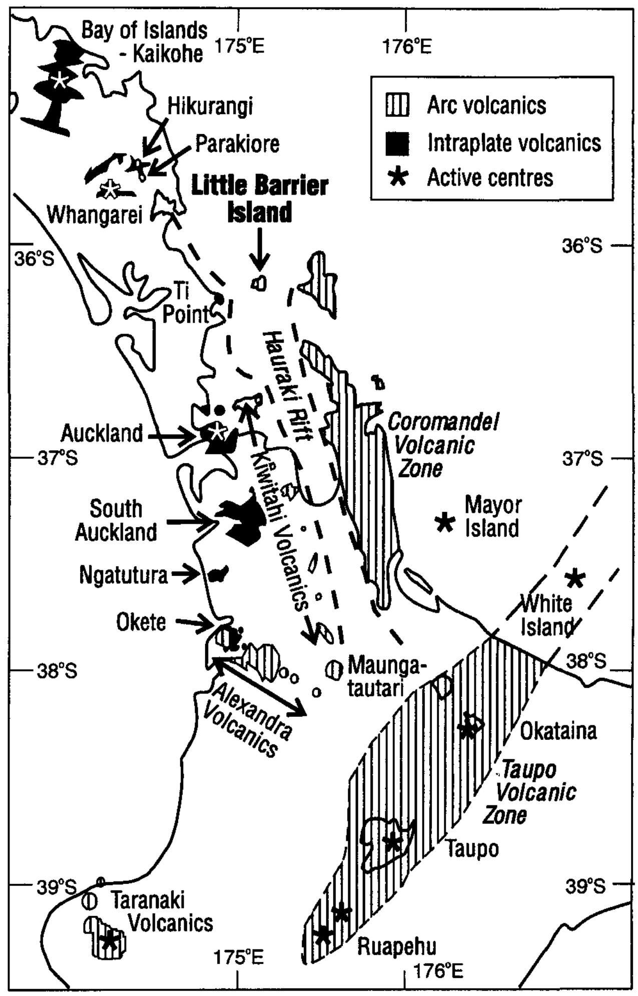

Fig. 1 Location of Little Barrier Island in the northern Hauraki Gulf. The distribution of mid-Miocene–Recent arc and intraplate volcanism is also shown.

G98003
Received 16 February 1998; accepted 18 February 1999

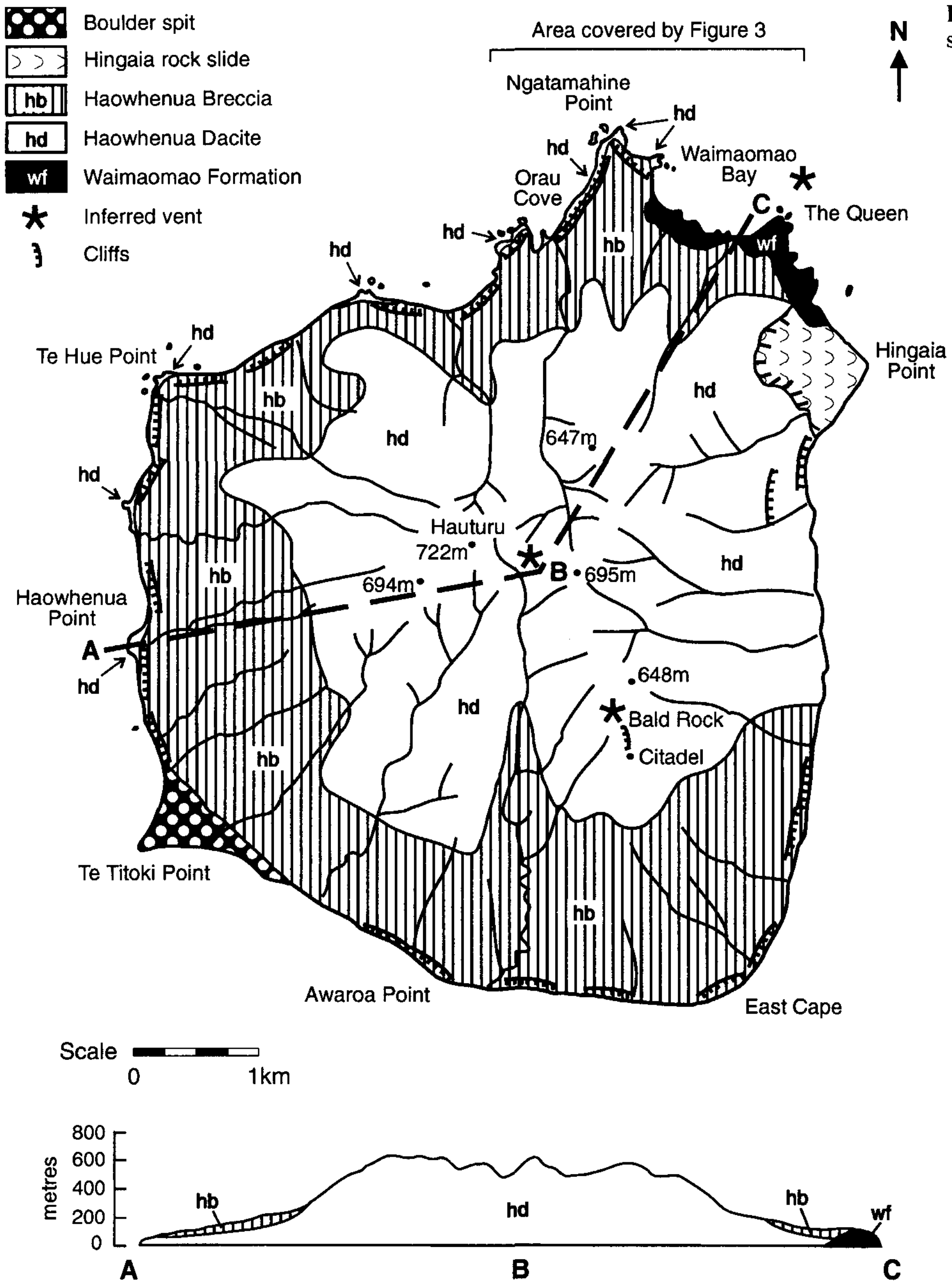

Fig. 2 Lithological map and cross-section of Little Barrier Island.

data from 64 samples. We also discuss the relationship of the volcano to the complex tectonic and magmatic environment of northern New Zealand.

GEOLOGY

Little Barrier Island is 7 km in diameter and rises to a summit 722 m above sea level (Fig. 2). The volcano extends a further 45 m below sea level, has a basal diameter of 8 km, and has a volume of c. 13 km^3. Outcrops on the island are mostly restricted to the coastal cliffs and summit peaks. A series of coastal lava flows, inland lavas, and a widespread breccia were recognised in all previous studies of the island, although slightly different stratigraphic schemes were erected (Table 1). We propose a new stratigraphic framework, based upon mapping of the island during 1993/94 and new age determinations (Table 2).

WAIMAOMAO FORMATION {wf}

Waimaomao Formation is a distinctive pinkish, strongly porphyritic rhyodacite with phenocrysts of plagioclase, hornblende, and traces of orthopyroxene that crops out along the northeastern coastline of the island. The type area is the coastal cliff behind Waimaomao Bay, where it forms a single homogeneous unit up to 150 m high (Fig. 2, 3). Spectacular flow banding is characteristic of the rhyodacite, and pronounced jointing orientated at 90° to the banding is developed in places. At the centre of the outcrop area, near a feature known as The Queen, the flow banding dips inward from both sides. Two samples of Waimaomao Formation have K-Ar ages of 2.9–3.1 Ma (Table 2). Twenty zircons extracted from one of these samples yielded a supporting U-Pb (SHRIMP) age of 3.1 ± 0.1 Ma (Table 2); older, inherited cores were not present in these zircons. The restricted area of the outcrop, thickness of the unit, and nature of the flow banding suggest that the rhyodacite is a small volcanic dome.

HAOWHENUA FORMATION

(modified from Kear 1961)

Haowhenua Dacite Member {hd}

Haowhenua Dacite is a dark grey, strongly porphyritic lava bearing phenocrysts of plagioclase, orthopyroxene, and traces of hornblende and augite. Flows of the dacite crop out at the base of cliffs along the western, northwestern, and eastern coast of the island. Few exposures reveal more than one flow, and typically the upper surface of these flows is oxidised to shades of purple and overlain by a dark red autobrecciated carapace that can be as much as 25 m thick (Fig. 3). The type locality is Haowhenua Point, where a +10 m thick flow is overlain by 15 m of autobreccia (Fig. 2). This outcrop was previously the type locality for Haowhenua Andesite (Kear 1961). Five samples of Haowhenua Dacite have K-Ar ages of 1.2–1.6 Ma (Table 2). Haowhenua Dacite appears to onlap Waimaomao Formation to the southeast of The Queen, but the contact area is inaccessible.

Outcrops of dark grey dacite also occur in the centre of the island, along incised stream valleys on the lower flanks of the cone, and in the 400 m high headscarp of the Hingaia Point rock slide (Fig. 2). Previously, these flows were grouped together as Hauturu Andesite (Kear 1961). They may have been fed by the resistant plugs and dikes of similar lava that crop out on the upper flanks of the cone and form distinct lineations (e.g., Bald Rock–Citadel, Fig. 2). Two samples from the inland outcrops have K-Ar ages of 1.4 and 1.5 Ma (Table 2). The ages of these samples and those of the coastal lavas overlap, and their petrography and geochemistry are identical. The inland lavas are interpreted simply as outcrops of the coastal lavas closer to their source, and are therefore part of Haowhenua Dacite.

Haowhenua Breccia Member {hb}

Haowhenua Breccia crops out along most of the coastline and along incised stream valleys on the lower flanks of the

Table 1 Reconciliation of the stratigraphic schemes erected by Hamilton (1937) and Kear (1961) with that proposed in this paper.

Hamilton (1937)	Kear (1961)		This paper	
	Hauturu Andesite		(= Haowhenua Formation: Haowhenua Dacite Member)	
Lava/fine-grained tuff				
Andesitic breccia		breccia		Haowhenua Breccia Member
	Haowhenua Formation:		Haowhenua Formation:	
Massive grey lava		andesite		Haowhenua Dacite Member
			------------ *1.4 m.y. hiatus* ------------	
			Waimaomao Formation:	rhyodacite

Table 2 Chronological database for Little Barrier Island. All K-Ar analyses were completed at Okayama University of Science (Takagi 1995); sample preparation and analytical techniques followed Briggs et al. (1989) and Itaya et al. (1991). Samples marked with an asterisk were collected by B. Hayward and their ages succinctly noted in Isaac et al. (1994). The U-Pb zircon analyses were completed at the Australian National University using the SHRIMP II; that analytical procedure is outlined in Compston et al. (1984) and Williams & Claesson (1987). Individual U-Pb dates are tabulated in Lindsay (1995). The decay constants listed in Steiger & Jager (1977) were used for K-Ar and U-Pb data reduction.

Sample (AU No.)	Location	Dated material	K (wt%)	^{40}Ar (radiogenic) (10^{-8} cm^3 g^{-1})	^{40}Ar (radiogenic) (%)	Age (Ma)
HAOWHENUA FORMATION: Haowhenua Dacite Member						
9024*	Near Bald Rock	whole rock	1.61	9.6	15	1.5 ± 0.2
9026*	Citadel	whole rock	1.55	8.2	12	1.4 ± 0.2
9027*	North of Lion Rock	whole rock	1.33	8.0	11	1.6 ± 0.3
9028*	Te Ananui–Te Hue	whole rock	1.50	8.7	11	1.5 ± 0.3
43812	Tirikakawa Stream	whole rock	1.50	8.9	50	1.5 ± 0.1
45433	Orau Cove	whole rock	1.34	6.5	15	1.2 ± 0.1
45434	Orau Cove	whole rock	1.59	9.9	46	1.6 ± 0.1
WAIMAOMAO FORMATION						
45435	Pohutukawa Flat	whole rock	2.22	25.5	58	3.0 ± 0.1
45436	Lots Wife	0.1 mm matrix	1.85	20.9	54	2.9 ± 0.1
		0.2 mm matrix	1.92	21.6	52	2.9 ± 0.1
		0.1 mm plagioclase	0.65	7.3	45	2.9 ± 0.1
		0.2 mm plagioclase	0.62	7.4	43	3.1 ± 0.1
45436	Lots Wife	average of 20 analysed zircons (^{238}U/^{206}Pb; SHRIMP)				3.1 ± 0.1

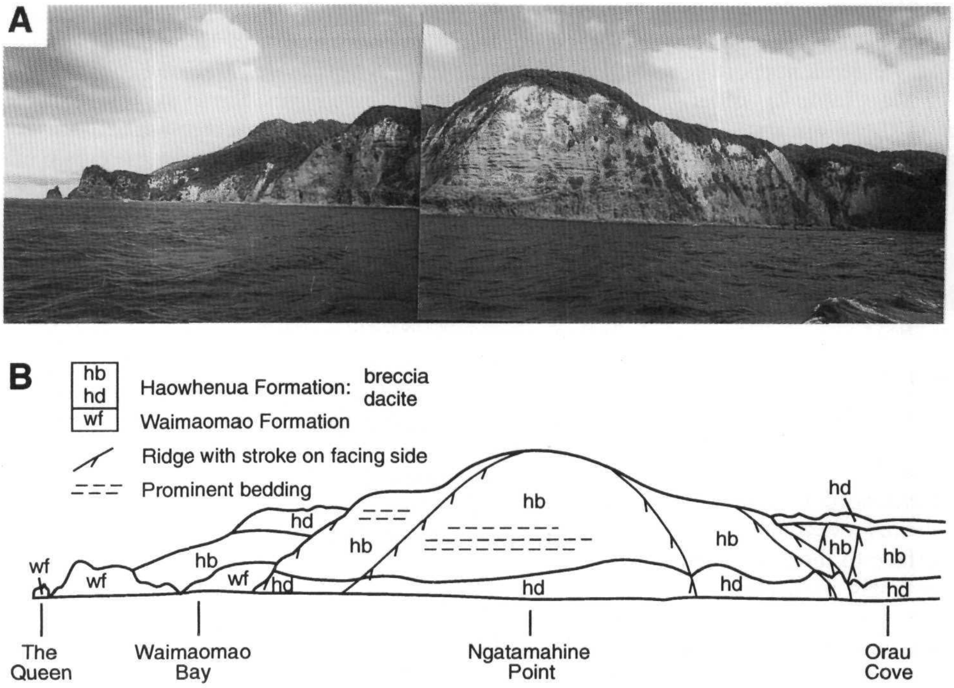

Fig. 3 A, Panorama of the northern coast from The Queen to Orau Cove (Fig. 2). **B**, Overlay showing the major units exposed along the coast and their stratigraphic relationships. The coastal cliff at Ngatamahine Point (photo centre) is 100 m high; a +5 m thick flow of Haowhenua Dacite crops out at the base of the cliff and is overlain by up to 25 m of oxidised autobreccia and 90 m of well-bedded Haowhenua Breccia. Waimaomao Formation in the cliff behind The Queen (photo left) is +150 m thick. Much of the island is surrounded by equally high coastal cliffs, and there is no evidence that these represent faults.

Fig. 4 Clast-supported Haowhenua Breccia at Awaroa Point consists of poorly bedded, variably altered dacitic lithics. Cap for scale.

cone. At the type area, near Ngatamahine Point, the breccia is >90 m thick and overlies Haowhenua Dacite (Fig. 3). This stratigraphic relationship is consistently seen where dacite flows and breccia are exposed along the coast. Haowhenua Breccia also appears to onlap Waimaomao Formation to the south of The Queen, but the contact is not accessible.

The breccia is usually well bedded, and consists of a succession of poorly sorted, ungraded, or reverse graded, 0.5–2.0 m thick beds. These beds are predominantly clast supported with a clay matrix. Clasts within each bed vary from subangular to subrounded and range from a few centimetres to >3 m in diameter. All clasts were derived from Haowhenua Dacite, but adjacent clasts show different degrees of alteration (Fig. 4), suggesting that they were derived from more than one area. Features characteristic of pyroclastic successions, such as interbedded fall and surge deposits, highly vesiculated clasts, breadcrust bombs, gas escape pipes, and post-depositional welding, are absent. From this evidence, we interpret the breccia as a stacked succession of stream-flood and debris-flow deposits. There is no indication of a significant time interval between the cessation of volcanism and the deposition of Haowhenua Breccia, and we accord it member status within Haowhenua Formation (Table 1).

PETROGRAPHY AND MINERALOGY

Waimaomao Formation is a strongly porphyritic rhyodacite (36–63% total phenocrysts), with phenocrysts of plagioclase (20–45%), hornblende (<5%), and traces of orthopyroxene set in a glassy groundmass (Table 3). Lavas of the Haowhenua Formation are similar, and consist of strongly porphyritic dacite (40–57% total phenocrysts) with phenocrysts of plagioclase (30–40%), orthopyroxene (1–8%), hornblende (<2%), and traces of augite set in a groundmass composed of plagioclase, orthopyroxene, and quartz with variable amounts of glass (Table 3). We interpret rare quartz crystals of phenocryst size as xenocrysts derived from crustal rocks, as Haowhenua Formation lavas do not bear alkali feldspar, biotite, or other phases that might suggest they evolved near the albite-orthoclase-quartz ternary minimum. Typically, Haowhenua Formation lavas contain more phenocrysts than those of Waimaomao Formation, although the total phenocryst content of lavas from both formations is highly variable. Small xenoliths of altered basaltic andesite are common in Waimaomao Formation but are seldom found in Haowhenua Formation.

Plagioclase is the most abundant phenocryst phase in all Little Barrier lavas, and forms euhedral crystals up to 0.8 mm in diameter that have either normal zoning from core to rim or oscillatory zoning patterns. The core compositions of these phenocrysts are mostly in the range An_{40-55} and their rim

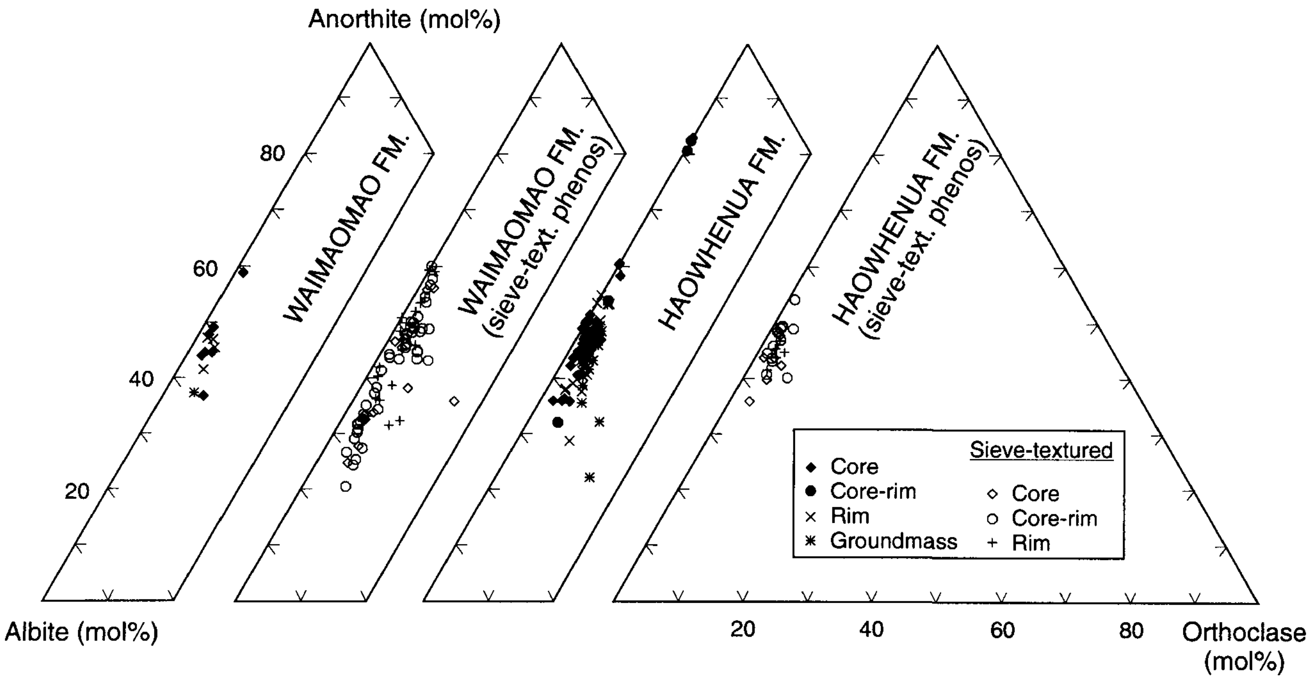

Fig. 5 Electron microprobe analyses of feldspar in 2 Waimaomao and 11 Haowhenua Formation lavas plotted within the anorthite-albite-orthoclase ternary diagram. Analyses were completed using a Jeol JXA-5A electron microprobe fitted with a Link LZ-5 energy dispersive detector and ZAF-4/FLS software. Each spectrum was collected for 100 s of live time using a beam diameter of 4 μm, a beam current of 0.3 nA, and an accelerating voltage of 15 kV.

compositions in the range An_{35-50} (Fig. 5). Approximately 25% of the plagioclase phenocrysts in Waimaomao Formation are much larger (up to 4 mm across) and are sieve textured. Their composition and zoning patterns are similar to those of the smaller phenocrysts, but they have a more calcic zone near their rims, and strong normal zoning is present from this calcic zone to the outer rim. The sieve-textured phenocrysts are rarer in Haowhenua Formation (2–5% of the plagioclase phenocrysts). Groundmass plagioclase microlite compositions are generally in the range An_{35-50}.

Hornblende is present in most Little Barrier lavas and occurs as elongate crystals up to 0.5 mm in length. Almost all hornblende phenocrysts are partly decomposed to fine-grained aggregates of opaque oxides and cryptocrystalline material, and many are completely pseudomorphed by these. This style of decomposition is a common characteristic of hornblende in lavas, and reflects the departure of the co-existing magma from the hornblende stability field as it ascends through the upper crust (Rutherford & Hill 1993). The complete breakdown of many large hornblende crystals suggests that at least part of the magma spent a considerable period of time (months to years) at depths shallower than 6.5 km before erupting. Analysed phenocrysts range from pargasitic hornblende to tschermakitic hornblende, and there is a marked decrease in their Mg number (100*Mg/[Mg+Fe]) from core to rim (76–55; Fig. 6).

Orthopyroxene is a minor phenocryst phase in all Little Barrier lavas and forms subhedral crystals up to 1 mm across. Many small orthopyroxene phenocrysts are partly oxidised and their relic cores are surrounded by rims of opaque or cryptocrystalline material. Where relic cores are absent, orthopyroxene pseudomorphs cannot be reliably distinguished from hornblende pseudomorphs. Orthopyroxene core compositions in Waimaomao Formation are predominantly in the range En_{65-80}, and rim compositions in the range En_{65-70}, whereas core compositions in Haowhenua Formation have lower Mg numbers and are in the range En_{55-75} with rim compositions mostly in the range En_{55-60} (Fig. 6).

Table 3 Representative modal analyses of Little Barrier lavas with phenocryst, pseudomorph, and groundmass contents reported in percentages. Fine-grained cryptocrystalline or opaque pseudomorphs may represent original hornblende or orthopyroxene. Each analysis consisted of 1000 counts on a 0.5 × 0.5 mm grid. "nd" denotes not detected.

Formation	Waimaomao		Haowhenua				
Sample (AU No.)	45436	46057	46066	46067	46074	46077	46088
Plagioclase	20.2	44.8	36.9	32.0	40.2	35.1	29.5
Hornblende	0.2	5.0	0.5	nd	1.8	0.2	0.3
Orthopyroxene	0.1	1.1	8.4	7.1	1.2	5.9	6.7
Clinopyroxene	nd	nd	0.6	nd	0.6	0.6	0.3
Fe-Ti oxide	6.0	2.0	3.9	5.0	2.2	1.1	3.1
Pseudomorphs	9.3	10.4	nd	7.6	10.5	7.8	nd
Groundmass	64.2	36.7	49.7	48.3	43.5	49.3	60.1

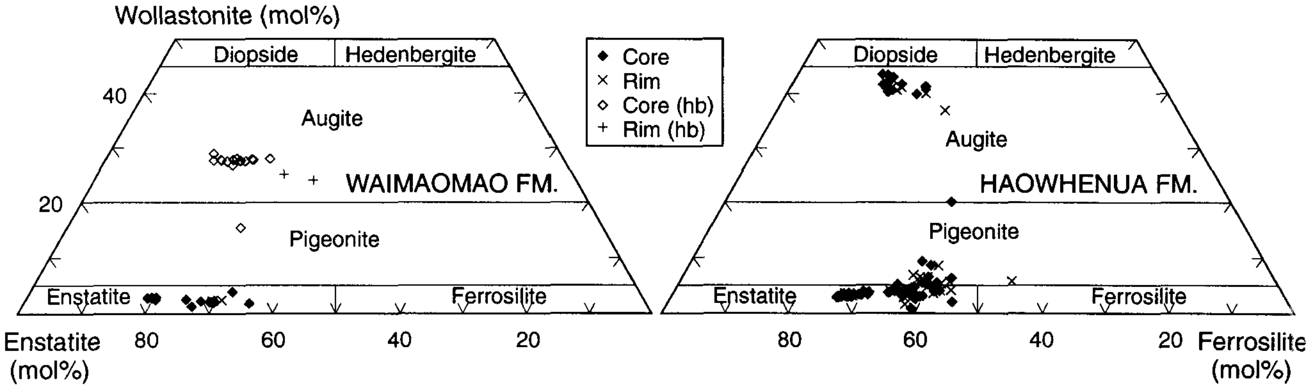

Fig. 6 Electron microprobe analyses of pyroxene in 1 Waimaomao and 10 Haowhenua Formation lavas plotted within the enstatite-diopside-hedenbergite-ferrosilite quadrilateral (fields after Morimoto et al. 1988). Hornblende analyses from a Waimaomao Formation lava are also projected into this system. Analytical conditions as for feldspar analyses (Fig. 5).

Small (<0.4 mm in diameter) augite phenocrysts occur only in Haowhenua Formation and have compositions in the range $En_{36-44}Fs_{14-27}Wo_{37-43}$. A crystallisation temperature of 1060°C was calculated for the rims of two intergrown pyroxene pairs in Haowhenua Formation using two-pyroxene geothermometry (Kretz 1982).

Accessory phases, typically <0.1 mm in length, include titaniferous magnetite, zircon (often corroded), and thin needles of apatite. Ilmenite is also present as an accessory phase in some Haowhenua Formation lavas.

GEOCHEMISTRY

Analytical methods

All samples from Little Barrier Island were scrubbed, leached in warm dilute HCl for 3 h, and then thoroughly washed with de-ionised water to remove any vestiges of sea spray. Major and trace elements were analysed by conventional X-ray fluorescence techniques using a Philips PW1410 spectrometer (Parker 1994a, b). Loss on ignition and H_2O^- were determined by gravimetry. For rare earth element (REE) analyses, 2 g of sample was dissolved in HF and a REE concentrate generated by cation exchange chromatography. The REE concentrate was analysed on an ARL 3410 inductively coupled plasma–atomic emission spectrometer, and the analytical precision was 3–5%. Representative raw analyses are reported in Table 4. Major element abundances cited in the text and shown on diagrams were recalculated to total 100 wt% on an anhydrous basis.

Four samples were analysed for Sr and Nd isotopic compositions by standard thermal ionisation mass spectrometry techniques at La Trobe University, Melbourne (Maas & McCulloch 1991). Mass fractionation effects were corrected on-line assuming $^{86}Sr/^{88}Sr = 0.1194$ and $^{146}Nd/^{144}Nd = 0.721903$. Laboratory averages for the NBS 987 Sr and La Jolla Nd standards were $^{87}Sr/^{86}Sr = 0.71024 \pm 0.00004$ and $^{143}Nd/^{144}Nd = 0.511857 \pm 0.000002$ (2σ), respectively, compared to accepted values of $^{87}Sr/^{86}Sr = 0.71024$ and $^{143}Nd/^{144}Nd = 0.511850$. Age corrections have not been applied; for the 3 m.y. old Waimaomao Formation $(^{87}Sr/^{86}Sr)_{Initial}$ may be 0.00004 lower than the value of $(^{87}Sr/^{86}Sr)_{Measured}$ reported in Table 4.

Results

Little Barrier lavas span the compositional range from dacite to rhyolite (63.8–70.8 wt% SiO_2), and can be classified as a medium-K series (Fig. 7). They have low Mg numbers (8–48; calculated assuming $Fe_2O_3/FeO = 0.2$), and generally have low to moderate concentrations of those elements that partition readily into the ferromagnesian silicates (e.g., Cr <35 ppm, Ni <20 ppm). All Little Barrier lavas have low concentrations of Ba (160–310 ppm) relative to dacite and rhyolite from the nearby Coromandel Volcanic Group (Fig. 7). Those from Haowhenua Formation, but not Waimaomao Formation, are also characterised by significantly lower concentrations of Rb (20–60 ppm) coupled with higher abundances of Zr (280–360 ppm) relative to Coromandel lavas of comparable SiO_2 content.

Lavas from Waimaomao Formation straddle the dacite–rhyolite boundary and are homogeneous within analytical error (69.9–70.8 wt% SiO_2). This is consistent with field evidence that suggests the formation is a single eruptive unit. In contrast, lavas from Haowhenua Formation form a compositional array of considerable range (63.8–69.2 wt% SiO_2), and for these lavas most analysed elements are negatively correlated with SiO_2; notable exceptions are K_2O, Rb, and Ba (Fig. 7). Waimaomao Formation lavas seldom plot on an extrapolation of the Haowhenua array, and the difference is especially marked for Sr and Zr (Fig. 7).

Unusually high chondrite normalised REE values (100–1000), coupled with negative Ce anomalies and high Y concentrations (100–1470 ppm), were obtained from several Little Barrier lavas that appeared fresh in both hand specimen and thin section. A similar phenomenon has been documented for some volcanic rocks from Hawaii (Roden et al. 1984; Foder et al. 1989), southeastern Australia (Price et al. 1991), and northern New Zealand (Kuschel & Smith 1992), and attributed to cryptic alteration. These samples were excluded from the database. The chondrite normalised REE patterns of all other Little Barrier lavas are characterised by light-REE enrichment relative to the heavy-REE, and negative Eu anomalies (Fig. 8). Light-REE enrichment is greater for lavas from Waimaomao Formation ($[La/Yb]_{Chon} = 8$) than for those of Haowhenua Formation ($[La/Yb]_{Chon} = 4$), and their Eu anomaly is more pronounced ($[Eu/Eu^*]_{Chon} = 0.66$ versus 0.82).

Normalisation of the Little Barrier analyses to the composition of an average mid-ocean ridge basalt (MORB) reveals that the large ion lithophile elements (LILE; e.g., K, Rb, Ba) are strongly enriched and decoupled from the high field strength elements (HFSE; e.g., Nb, Zr, Yb), with the latter being weakly enriched or comparable to MORB (Fig. 9). This type of pattern is typical of subduction-related magmas (Pearce 1982), though they often have a small negative Nb anomaly. Lavas from Waimaomao Formation have higher LILE and lower HFSE concentrations ($[Rb/Zr]_{MORB} = 67$, $[Rb/Yb]_{MORB} = 309$) than those of Haowhenua Formation ($[Rb/Zr]_{MORB} = 8$, $[Rb/Yb]_{MORB} = 37$).

The isotopic composition of Sr and Nd in four Little Barrier lavas is variable (e.g., $^{87}Sr/^{86}Sr = 0.7036–0.7040$), but comparable to that of basalt from the Tonga–Kermadec intra-oceanic arc. All analysed lavas are considerably less radiogenic than both basalt-andesite and rhyolite from the Taupo Volcanic Zone (Fig. 10, Table 4). Lavas from both Waimaomao and Haowhenua Formations have similar $^{87}Sr/^{86}Sr$ and $^{143}Nd/^{144}Nd$ values. There is no obvious correlation of $^{87}Sr/^{86}Sr$ with SiO_2 or other geochemical parameters, although the number of analyses is small.

DISCUSSION

Both the tectonic and magmatic settings of Little Barrier are complex. The volcano is located in the central part of the late Miocene–Recent Hauraki Rift, which is presently regarded as an amagmatic intra-continental rift (Hochstein & Ballance 1993). To the west, late Miocene–Recent intraplate basalt and its derivatives have erupted from a series of volcanic fields on the Northland Peninsula, and small outcrops of older mid-Miocene basalt with both arc and

Table 4 Representative whole rock geochemistry of Waimaomao and Haowhenua Formations, with major elements reported in wt%, trace elements in ppm, and "nd" denoting below detection limit. The full database includes 64 major and trace element analyses, and 17 REE analyses (Lindsay 1995). "Xeno." is a xenolith from a Waimaomao Formation lava, whereas "Hiku." and "Para." are lavas from Hikurangi and Parakiore domes near Whangarei (see discussion).

	Waimaomao		Haowhenua										
Unit											Xeno.	Hiku.	Para.
AU No.	46060	45436	45433	46081	46066	43814	46094	46084	45434	46072	46078	45479	18799
SiO_2	69.08	69.27	62.98	63.05	64.03	65.53	65.84	66.41	67.65	68.29	53.51	68.50	67.22
TiO_2	0.50	0.50	0.72	0.76	0.71	0.66	0.67	0.63	0.59	0.54	0.97	0.42	0.41
Al_2O_3	15.44	15.69	16.18	16.38	16.23	15.68	16.19	15.71	15.87	15.31	20.59	16.93	15.53
Fe_2O_3	2.66	3.16	5.31	5.73	5.09	4.74	4.81	4.63	4.00	3.95	8.04	3.37	2.92
MnO	0.02	0.06	0.09	0.11	0.13	0.10	0.11	0.10	0.07	0.08	0.12	0.12	0.08
MgO	0.29	0.44	2.09	1.75	1.64	1.80	1.09	1.43	0.61	1.19	2.68	0.30	0.53
CaO	2.63	2.73	4.59	4.69	4.44	4.35	3.97	4.13	3.65	3.40	8.23	1.74	2.39
Na_2O	4.53	4.54	4.39	4.83	4.17	4.60	4.40	4.48	4.54	4.19	3.30	5.05	4.84
K_2O	2.36	2.42	1.37	1.03	1.59	1.28	1.34	1.34	1.65	1.77	0.45	2.06	2.29
P_2O_5	0.13	0.24	0.34	0.37	0.27	0.26	0.25	0.23	0.21	0.19	0.29	0.07	0.15
H_2O^-	1.49	0.16	0.37	0.33	0.40	0.25	0.88	0.26	0.38	0.23	0.47	0.36	0.52
LOI	0.66	0.75	1.59	0.77	1.34	0.62	0.61	0.73	0.77	0.81	0.81	1.48	2.48
Total	99.77	99.94	100.01	99.77	100.01	99.84	100.14	100.06	99.96	99.91	99.44	100.40	99.40
V	46	33	73	78	74	74	61	67	59	54	144	11	15
Cr	18	18	31	21	14	16	12	18	6	27	10	5	4
Ni	11	7	16	11	4	11	6	9	nd	11	nd	3	4
Cu	8	6	14	12	11	14	6	12	9	12	95	nd	nd
Zn	39	26	72	73	73	62	65	59	51	50	86	50	65
Rb	89	95	24	23	34	30	33	35	49	58	8	57	65
Sr	256	254	229	206	187	177	180	176	169	157	551	163	202
Y	25	20	37	39	46	38	33	33	31	28	25	24	33
Zr	197	188	331	357	325	304	314	304	300	289	137	300	280
Nb	11	10	13	12	12	10	10	10	10	10	8	14	12
Ba	296	306	199	168	183	193	207	215	239	242	131	409	357
Pb	13	20	7	9	9	11	9	10	8	12	7	16	17
Th	11	12	nd	5	nd	5	4	6	3	6	nd	12	9
La		19.5	20.6	20.2	21.0		19.0	19.3	17.9	17.4			
Ce		39.0	42.0	43.4	43.9		42.0	40.4	35.6	35.5			
Pr		4.6	5.6	5.4	5.6		5.7	4.7	4.9	4.5			
Nd		16.5	23.0	22.5	22.0		23.0	19.8	18.5	18.0			
Sm		3.5	5.1	5.2	5.1		4.9	4.5	4.2	4.1			
Eu		0.7	1.3	1.4	1.3		1.2	1.1	1.1	1.1			
Gd		3.1	5.3	5.5	5.6		4.7	4.6	4.2	4.2			
Dy		3.0	5.3	5.7	6.0		4.9	4.6	4.4	4.2			
Er		1.7	3.1	3.8	3.7		2.9	3.3	2.7	2.5			
Yb		1.7	3.1	3.3	3.6		3.0	2.8	2.6	2.4			
Lu		0.3	0.5	0.6	0.6		0.5	0.5	0.4	0.4			
$^{87}Sr/^{86}Sr$		0.70373		0.70355		0.70371			0.70396				
$^{143}Nd/^{144}Nd$		0.512935		0.513029		0.512986			0.512971				
εNd		5.8		7.6		6.8			6.5				

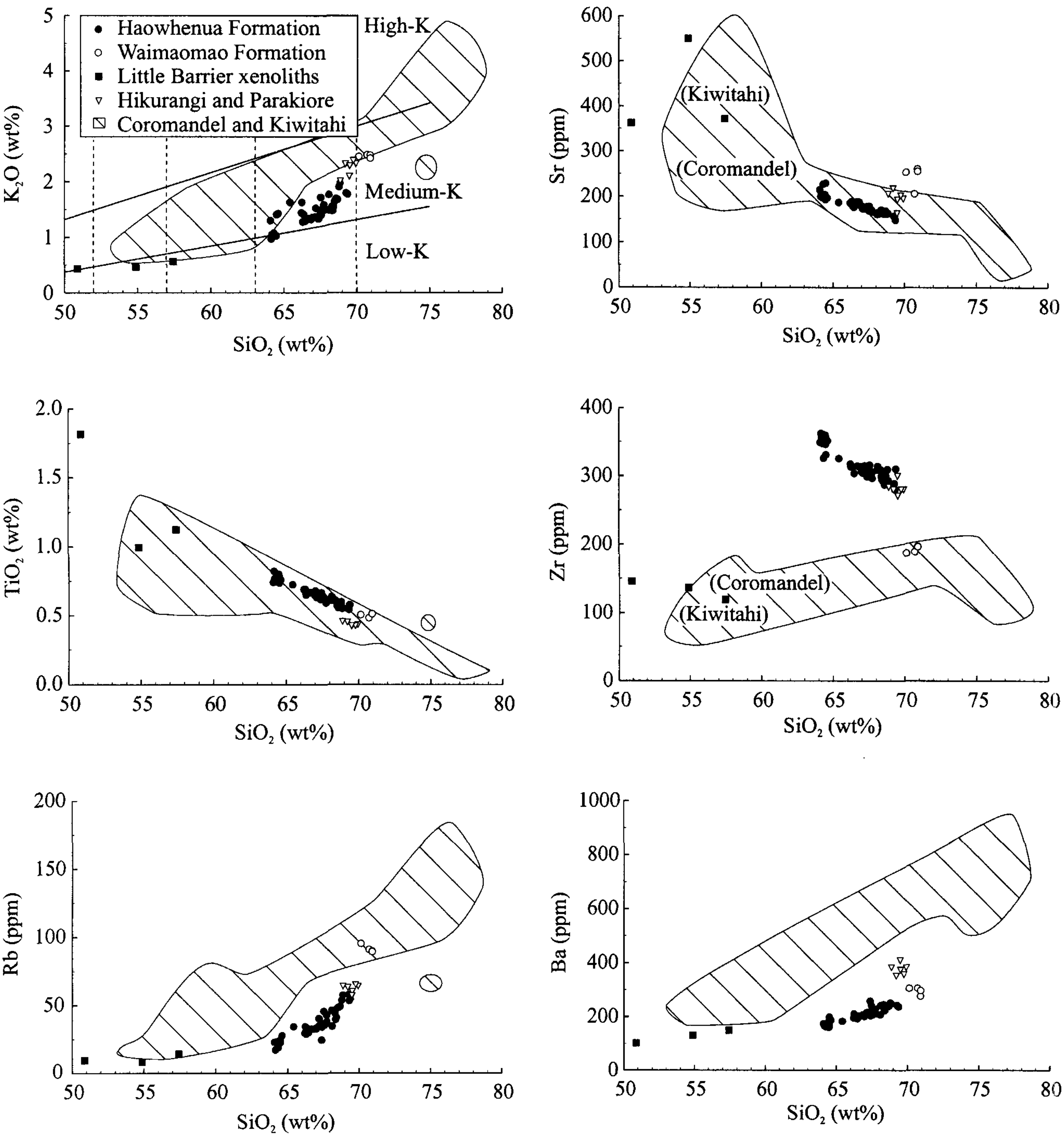

Fig. 7 Selected Harker diagrams for Little Barrier lavas and xenoliths. Also shown are analyses of Hikurangi and Parakiore lavas referred to in the discussion (PM Black, 6 unpublished analyses), and the compositional field for the Coromandel Volcanic Group (IEM Smith, 95 unpublished analyses) and the Kiwitahi Volcanics (Black et al. 1992).

intraplate geochemical characteristics have also been identified (Smith 1989; Smith et al. 1993). Little Barrier is younger than the Miocene–Pliocene subduction-related magmatism of the nearby Coromandel Volcanic Group and the associated Kiwitahi Volcanics (Black et al. 1992; Adams et al. 1994), although the Haowhenua Formation is contemporaneous with the oldest subduction-related volcanism in the Taupo Volcanic Zone, 200 km to the south (Wilson et al. 1995). In this discussion, we explore the relationship of Little Barrier to these features and to the complex rearrangement of the subduction system through northern New Zealand between 4 and 1.5 Ma.

Geochemical affinity

Little Barrier lavas share few geochemical features of the intraplate lavas erupted on the Northland Peninsula. The latter mostly comprise basaltic rocks ranging from alkali basalt to tholeiite with high concentrations of both the LILE and HFSE. For example, at 45 wt% SiO_2, the intraplate lavas have >1 wt% K_2O, >200 ppm Ba, >35 ppm Nb, and their

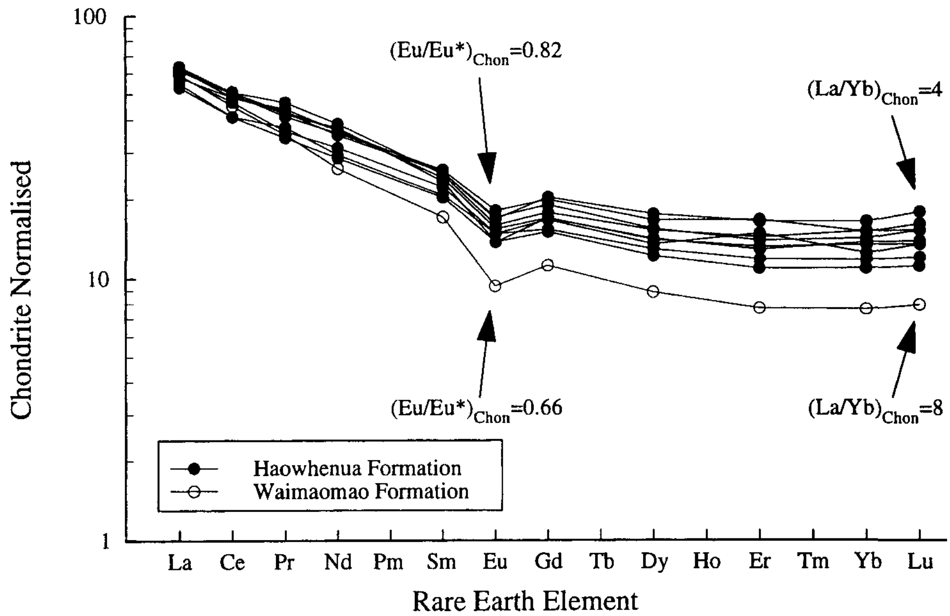

Fig. 8 Chondrite normalised REE diagram for representative Little Barrier lavas. Lavas from Waimaomao Formation have a steeper pattern and a larger negative Eu anomaly than those of Haowhenua Formation. Normalisation factors after Nakamura (1974).

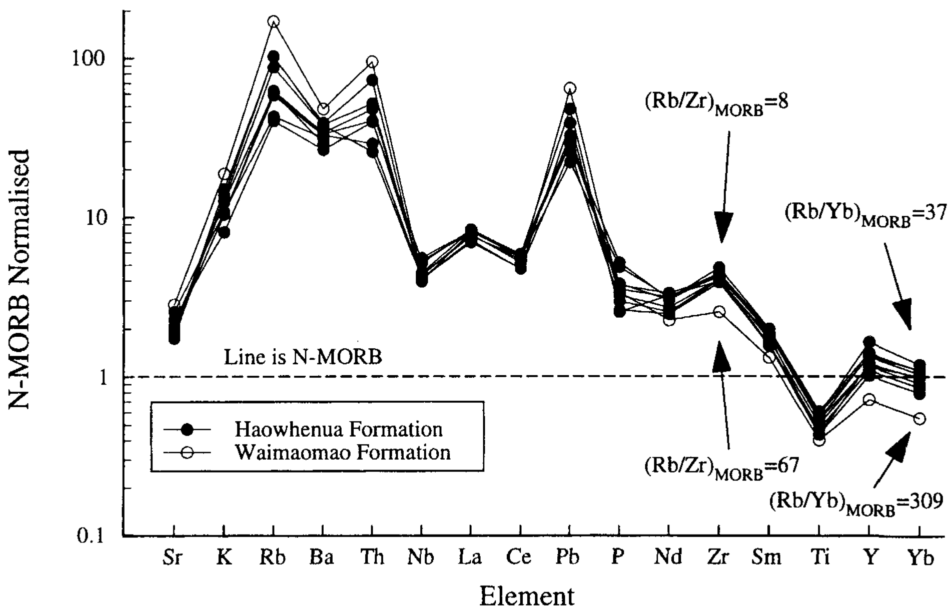

Fig. 9 MORB normalised diagram for representative Little Barrier lavas. All lavas are strongly enriched in the LILE. However, the extent of decoupling between the LILE and the HFSE is greater for lavas from Waimaomao Formation than for those of Haowhenua Formation. Normalisation factors after Pearce & Parkinson (1993).

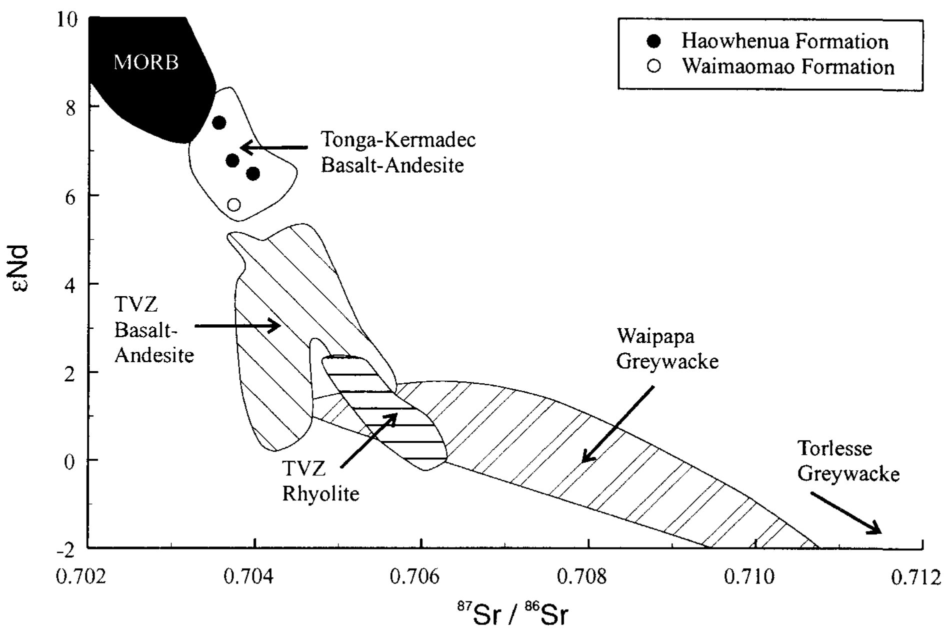

Fig. 10 Radiogenic Sr and Nd isotopic compositions of Little Barrier lavas compared to MORB and the nearby volcanic rocks of the Tonga–Kermadec intra-oceanic arc and the Taupo Volcanic Zone. Also shown are arrays for the Waipapa and Torlesse greywacke basement rocks of northern New Zealand. Fields after Graham et al. (1995).

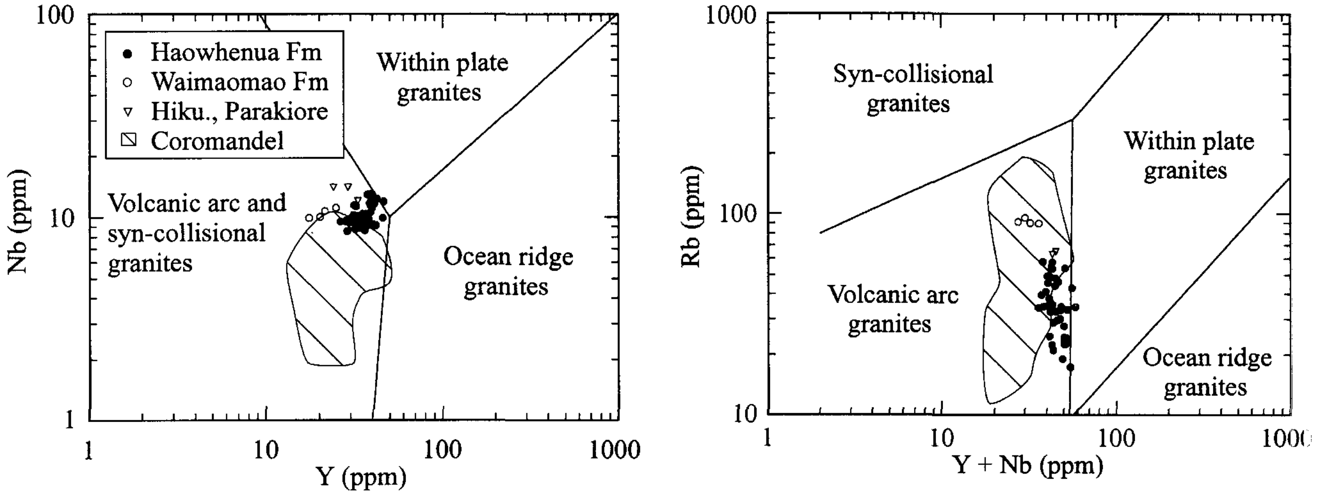

Fig. 11 Tectonic discrimination diagrams for felsic rocks. Lavas from Little Barrier, Hikurangi, Parakiore, and the Coromandel Volcanic Group mostly plot within the volcanic arc granite field on each diagram. Fields after Pearce et al. (1984).

chondrite normalised REE patterns are strongly light REE enriched with $(La/Yb)_{Chon} > 10$ (data from Huang et al. 1997). Magma of this composition may evolve to rhyolite by fractional crystallisation, but the resulting liquid is peralkaline with extremely high LILE and HFSE concentrations (e.g., Nb >150 ppm; Smith et al. 1977).

In contrast, the decoupling of the LILE and HFSE in Little Barrier lavas is a typical signature of subduction-related magmas (Pearce 1982). Furthermore, Little Barrier lavas plot within the volcanic arc granite field on tectonic discrimination diagrams for felsic rocks (Fig. 11). The older Waimaomao Formation is indistinguishable from dacite and rhyolite of the Coromandel Volcanic Group for many major and trace elements (Fig. 7), although the Haowhenua Formation lavas are geochemically distinct from these. A decrease in the subduction-related component with time is indicated by the decrease in chondrite normalised light REE enrichment from Waimaomao Formation lavas to those of Haowhenua Formation (Fig. 8), the smaller degree of LILE and HFSE decoupling in Haowhenua Formation lavas (Fig. 9), and the position of Haowhenua Formation lavas adjacent to the volcanic arc granite to within plate granite boundary on the tectonic discrimination diagrams (Fig. 11). These observations lead us to the opinion that Little Barrier is related to the termination of the subduction-related magmatism represented by the Coromandel Volcanic Group.

Petrogenesis of the Haowhenua Dacite

Conventional models of subduction-related magma genesis envisage a critical role for both the subducting plate and the overlying mantle wedge; the former is the source of an aqueous fluid enriched in the LILE, whereas the latter undergoes partial melting in response to fluxing by the fluid (e.g., Tatsumi et al. 1986; Pearce & Peate 1995). Therefore, primary arc magmas should be basaltic in composition because they are mantle melts. If Little Barrier lavas are subduction related, it is reasonable to expect that the original magma must have evolved from basalt to dacite and rhyolite by some combination of fractionation processes. We can dismiss both crustal assimilation and crustal anatexis as significant processes because Little Barrier lavas have intra-oceanic arc-like $^{87}Sr/^{86}Sr$ and $^{143}Nd/^{144}Nd$ isotope values (Fig. 10), whereas the crust beneath Little Barrier is composed of Waipapa Terrane greywacke with relatively radiogenic $^{87}Sr/^{86}Sr$ and $^{143}Nd/^{144}Nd$ isotope values (Graham et al. 1992).

There are no outcrops of basalt within 25 km of Little Barrier Island. However, a possible basaltic parent magma is represented by a xenolith from the Haowhenua Formation (AU46078, Table 4). The concentration of incompatible trace elements in the least evolved Haowhenua Dacite (AU46081 Table 4) was modelled by fractional crystallisation of the basaltic xenolith using the Rayleigh fractionation equation $C_L = C_O F^{(D-1)}$, where C_L is the concentration in the derivative magma, C_O is the concentration in the parent magma, F is the fraction of magma remaining, and D is the bulk distribution coefficient for the element in the extract assemblage (Rollinson 1993). Calculated values of F were 0.35 for Rb, 0.38 for Zr, 0.44 for K, 0.64 for Y, and 0.78 for Ba, assuming each of these elements was totally incompatible in the extract assemblage ($D = 0$). In practice, F values for K, Y, and Ba can be reduced to agree with those calculated for Rb and Zr by allowing plagioclase and hornblende to dominate the extract assemblage. This reflects significant partitioning of K, Y, and Ba into plagioclase and hornblende, resulting in $D > 0$ for those elements. However Ba is less compatible in hornblende than K, whereas both elements have similar compatibility in plagioclase (Rollinson 1993). Therefore, any successful model must feature a parent magma with higher K/Ba than basaltic xenolith AU46078

Rubidium is the most incompatible element we have analysed in Little Barrier lavas, and thus provides the most reliable constraint on the true value of F. The Rb concentration of the least evolved Haowhenua Dacite is attained after 65% crystallisation of the parent basaltic magma in the model. This is comparable to that proposed for other andesite–dacite lavas (e.g., Ruapehu; Graham & Hackett 1987). Substituting primitive basalt compositions from the Taupo Volcanic Zone into the model does not significantly change this result. Most Taupo Volcanic Zone

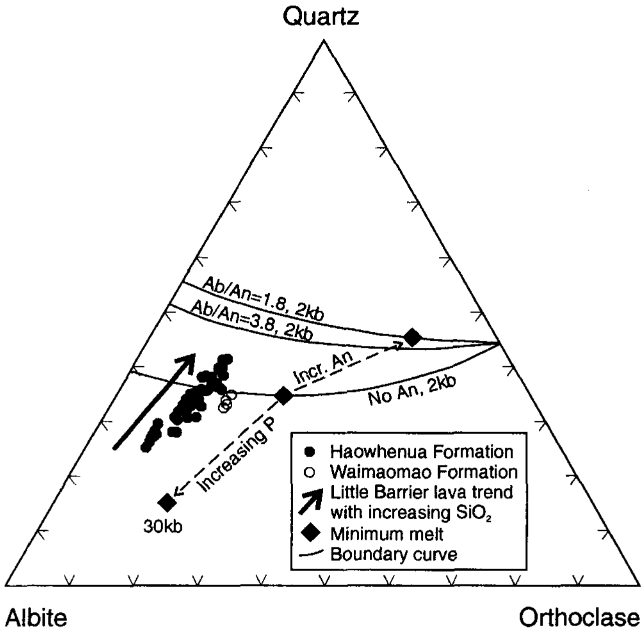

Fig. 12 Little Barrier lavas plotted in the normative albite-orthoclase-quartz ternary system. Boundary curves are shown for $P(H_2O)$ = 2 kbar at albite/anorthite values of 1.8, 3.8, and ∞. The effect on the minimum melt composition of increasing P and the albite/anorthite value is also indicated. Haowhenua Formation and Waimaomao Formation lavas have albite/anorthite values in the range 1.7–4.0, trend towards the quartz apex with increasing SiO_2 content, and show no sign of reaching the plagioclase-quartz boundary curve. Phase relationships after von Platen (1965).

basalts (e.g., TVZ-15 of Gamble et al. 1993) have similar or lower Rb concentrations than the basaltic xenolith, and therefore must undergo similar or greater amounts of crystallisation to produce Little Barrier dacite. However, all outcrops on Little Barrier consist of dacite or more siliceous lava, and the total volume of the volcano is 13 km^3. If the entire volcano is built of dacite, >35 km^3 of a parent basaltic magma is required, and a gabbroic cumulate complementary to the dacite would reside in the crust. This is evidence that Little Barrier represents a large magmatic system that cannot be dismissed as a small isolated anomaly.

Further insights into the petrogenesis of Little Barrier lavas were obtained by modelling the geochemical variation within the Haowhenua Formation. These lavas have a considerable range of dacitic compositions and form linear arrays when plotted on Harker diagrams (Fig. 7). Following the procedure adopted in the previous section, the Rb concentration in the most evolved Haowhenua Dacite was modelled by a further 59% fractional crystallisation of the least evolved dacite (parent = AU46081, Rb = 22.5 ppm; daughter = AU46079, Rb = 54.5 ppm). This result, $F = 0.41$, was then used to constrain major element mass balance models in which the modal composition of the extract assemblage and the mineral compositions were allowed to vary (Table 5). A range of non-unique models was generated in which the sum of the least squares residuals was very low. The model whose modal and phenocryst compositions most closely resembled that of the Haowhenua Dacite had an extract assemblage consisting of 71% plagioclase, 12% quartz, 9% orthopyroxene, and minor clinopyroxene, titaniferous magnetite, apatite, ilmenite, and zircon.

The goodness of fit in such models is a reflection of the large number of phases in the extract assemblage. Indeed, it would be remarkable if no model of this type could generate a close fit. At issue is whether the proportions of each phase and their compositions are realistic. In this instance, the requirement for 12% quartz in the extract assemblage severely limits the credibility of the model. Large quartz crystals were identified in few thin sections, always totalled <1% of the mode, and were interpreted as xenocrysts. Furthermore, Haowhenua Formation lavas trend towards the quartz apex on a normative albite-orthoclase-quartz plot, and are far to the plagioclase side of the plagioclase-quartz boundary curve at $P(H_2O)$ = 2 kbar and albite/anorthite values in the range 2–4 (Fig. 12). Thus, quartz should not be a crystallising phase in Haowhenua Dacite. Alternative models in which hornblende replaces some portion of pyroxene + plagioclase in the extract assemblage require more quartz to fractionate. The amount of quartz could be

Table 5 Major element fractional crystallisation model for the generation of the most evolved Haowhenua Dacite (AU46079) from the least evolved (AU46081). The weight fraction of each phase is given, together with the percentage of each mineral in the extract assemblage and its composition. Although the sum of the least squares residuals is very low, the real issue is whether the phase proportions and compositions are realistic (see text). Zircon is also known to be a fractionating phase (e.g., the decrease in Zr with increasing SiO_2 on Fig. 7), but its effect on the model is negligible (0.05 wt% ZrO_2 → 0.04 wt% ZrO_2).

	Parent	Phases in the extract assemblage							Daughter	
	AU46081	Plagioclase	Quartz	Orthopyroxene	Clinopyroxene	Magnetite	Ilmenite	Apatite	Model	AU46079
wt fraction	1.00	0.42	0.06	0.05	0.02	0.02	0.01	0.01	0.41	
% of extract		71	12	9	3	3	1	1		
SiO_2	63.88	60.08	100.00	51.11	51.20	0.33	0.32		69.14	69.14
TiO_2	0.77			0.35	0.35	11.92	45.82		0.55	0.56
Al_2O_3	16.60	23.80		0.89	1.11	0.80			15.88	15.86
Fe_2O_3	5.81	1.48		24.42	13.73	86.08	51.90		3.85	3.86
MnO	0.11			0.92	0.62	0.39	0.72		0.10	0.09
MgO	1.77			21.09	13.02	0.48	1.24		1.09	1.08
CaO	4.75	6.39		1.22	19.29			56.00	3.22	3.20
Na_2O	4.89	7.46			0.68				4.27	4.29
K_2O	1.04	0.79							1.70	1.72
P_2O_5	0.38							44.00	0.20	0.20
		An_{31}		En_{62}	En_{39}					
		Ab_{65}		Fs_{35}	Fs_{20}					
		Or_4		Wo_3	Wo_{41}					

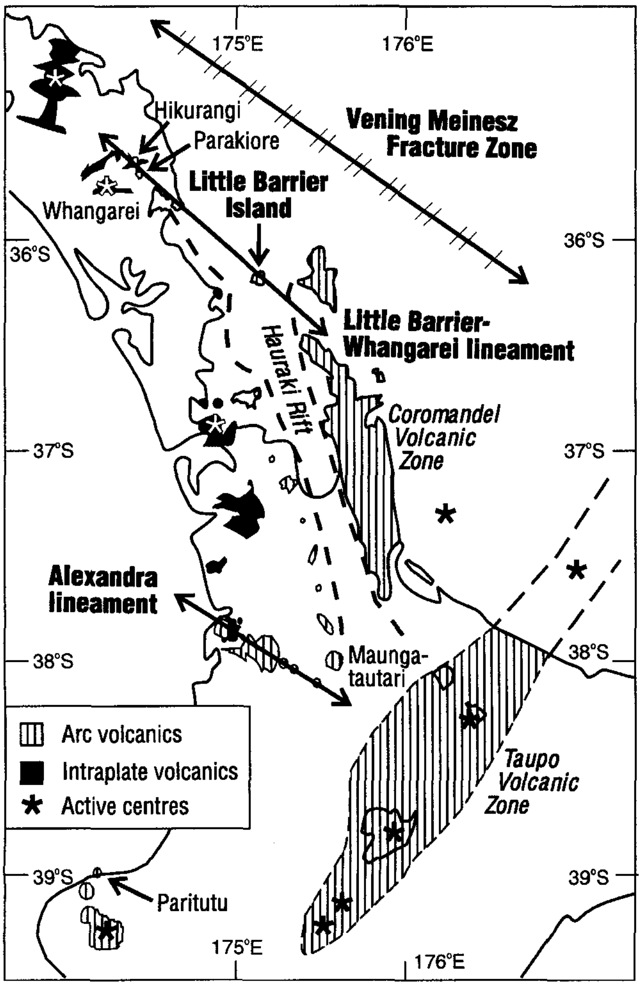

Fig. 13 Late Pliocene–Pleistocene volcanic lineaments in northern New Zealand. Geochemically distinctive volcanoes erupted along both the Little Barrier–Whangarei and Alexandra lineaments as subduction-related volcanism migrated from the Coromandel Peninsula to the Taupo Volcanic Zone. Both lineaments are subparallel to the continental margin, marked by the Vening Meinesz Fracture Zone.

reduced if less titaniferous magnetite or ilmenite were crystallised, but then the Ti and Fe contents of pyroxene (or hornblende) must increase to levels far higher than those observed. A second problem is the plagioclase composition of An_{31}. This is more sodic than groundmass plagioclase (An_{40-45}) in the Haowhenua Dacite, although similar to the most sodic zones of the large sieve-textured plagioclase phenocrysts. Increasing the An content of plagioclase in the extract assemblage requires more quartz to fractionate.

Closed-system fractional crystallisation models are probably too simple for long-lived large magmatic systems such as Little Barrier. More likely, batches of magma ponded within the crust, underwent variable amounts of fractional crystallisation, and were intermittently recharged by more primitive magma from below. Mixing of a hot primitive magma with a cooler dacitic magma should cause resorption of the phenocrysts in the latter. Little Barrier lavas commonly have sieve-textured plagioclase phenocrysts with near-rim calcic zones, and at other volcanoes these have been interpreted as evidence of either recharge or magma mixing events (e.g., Hibbard 1981; Graham & Worthington 1988; Stimac & Pearce 1992). We suspect that these processes also occurred at Little Barrier. A consequence of such open-system behaviour is that the major and trace element concentrations can decouple from each other (O'Hara & Mathews 1981), leading to spurious requirements for the extract assemblage if closed-system fractional crystallisation models are applied.

In conclusion, simple fractionation models in which a primitive arc-type magma is parental to the Haowhenua Dacite are not easily reconciled with the observed phase assemblages or with the geochemistry of the dacite. However, more complex open-system fractionation-recharge-mixing models may provide an alternative that can overcome these obstacles. Little Barrier Island represents a small portion of this intriguing magmatic system, and we are unable to fully resolve its petrogenesis from the available data.

The Little Barrier–Whangarei lineament

Subduction-related volcanism on Coromandel Peninsula ceased at 4.2 Ma (Adams et al. 1994) and commenced in the Taupo Volcanic Zone between 2.0 and 1.5 Ma (Wilson et al. 1995). The interval 4.2–1.5 Ma marks a complex transition period, during which subduction-related volcanism migrated southwards from the southeastern Coromandel Peninsula through the Kaimai–Tauranga region and into the Taupo Volcanic Zone. Elsewhere, a significant volume of subduction-related magma was erupted between 2.7 and 1.6 Ma to form the Alexandra Volcanics, a linear chain of volcanoes that trend 300° (Briggs et al. 1989), and lesser volumes were erupted at Maungatautari (Briggs 1986) Paritutu (Neall et al. 1986), and Little Barrier Island (Fig. 13). The relationship of these centres to each other, or to a subducting slab, is obscure.

Near the end of this transition period, two young dacite domes were extruded near Whangarei (Fig. 13). These domes are slightly younger than the Haowhenua Dacite of Little Barrier; Hikurangi has a K-Ar age of 1.2 ± 0.1 Ma and Parakiore an age of 0.8 ± 0.1 Ma (Takagi 1995). Lavas from these two domes are geochemically similar to the Haowhenua Dacite, and overlap the high-SiO_2 end of the Haowhenua array on most Harker diagrams (Table 4; Fig. 7). They are the only lavas in northern New Zealand that share the distinctive Zr-rich, Rb- and Ba-poor signature of the Haowhenua Dacite. Therefore, we suggest the origin of these domes and that of the Haowhenua Dacite are linked.

A line drawn between Little Barrier Island and Hikurangi passes through Parakiore and may delineate the northern limit of the active Hauraki Rift (Fig. 13). This lineament trends 310° and is subparallel to that of the Alexandra Volcanics. Furthermore, the lineament is also subparallel to the Vening Meinesz Fracture Zone, which marks the boundary between the continental crust of New Zealand and the oceanic crust to the north. The 900 km long Vening Meinesz Fracture Zone is a 100 km wide deformation zone that has been a feature of the continental margin since at least the early Miocene, and has a complex record of strike slip and transpressional motion with both dextral and sinistral displacement (Herzer & Mascle 1996).

The Little Barrier–Whangarei and the Alexandra lineaments could represent crustal fractures parallel to the Vening Meinesz Fracture Zone. Minor extension across these fractures during the Pliocene–Pleistocene realignment of the plate margin may have allowed the last vestiges of magma generated by the subducting slab associated with the Miocene to early Pliocene volcanism on Coromandel Peninsula to intrude the crust and erupt. This would also explain the decreasing subduction signature with time in Little Barrier lavas.

ACKNOWLEDGMENTS

Detailed and constructive reviews by John Gamble and an anonymous referee led to a significantly improved manuscript, and we thank them for their time and efforts. JML gratefully acknowledges the assistance of the Department of Conservation staff based on Little Barrier during 1993/94. We also thank Roger Briggs, Tetsu Itaya, and Miki Takagi for their interest and help with the initial fieldwork, and Tetsu and Miki again for the K-Ar age determinations. The U-Pb SHRIMP ages were determined by JML as part of a Vacation Scholarship project at the Research School of Earth Sciences, ANU. The Sr and Nd isotope analyses were made possible by a University of Auckland Research Committee Grant to PMB.

REFERENCES

Adams, C. J.; Graham, I. J.; Seward, D.; Skinner, D. N. B. 1994: Geochronological and geochemical evolution of late Cenozoic volcanism in the Coromandel Peninsula, New Zealand. *New Zealand Journal of Geology and Geophysics 37*: 359–379.

Black, P. M.; Briggs, R. M.; Itaya, T.; Dewes, E. R.; Dunbar, H. M.; Kawasaki, K.; Kuschel, E.; Smith, I. E. M. 1992: K-Ar age data and geochemistry of the Kiwitahi Volcanics, western Hauraki Rift, North Island, New Zealand. *New Zealand Journal of Geology and Geophysics 35*: 403–413.

Briggs, R. M. 1986: Petrology and geochemistry of Maungatautari, a medium-K andesite-dacite volcano. *New Zealand Journal of Geology and Geophysics 29*: 273–289.

Briggs, R. M.; Itaya, T.; Lowe, D. J.; Keane, A. J. 1989: Ages of the Pliocene–Pleistocene Alexandra and Ngatutura Volcanics, western North Island, New Zealand, and some geological implications. *New Zealand Journal of Geology and Geophysics 32*: 417–427.

Compston, W.; Williams, I. S.; Meyer, C. 1984: U-Pb geochronology of zircons from lunar breccia 73217 using a sensitive high mass-resolution ion microprobe. *Journal of Geophysical Research 89*: 525–534.

Foder, R. V.; Malta, D. P.; Bower, G. R.; Jacobs, R. S. 1989: Microprobe analyses of rare earth phosphate in basalt from Kahoolawe Island, Hawaii. Proceedings of the 24th annual conference, Microbeam Analytical Society. Pp. 554–558.

Gamble, J. A.; Smith, I. E. M.; McCulloch, M. T.; Graham, I. J.; Kokelaar, B. P. 1993: The geochemistry and petrogenesis of basalts from the Taupo Volcanic Zone and Kermadec Island Arc, S.W. Pacific. *Journal of Volcanology and Geothermal Research 54*: 265–290.

Graham, I. J.; Hackett, W. R. 1987: Petrology of calc-alkaline lavas from Ruapehu Volcano and related vents, Taupo Volcanic Zone, New Zealand. *Journal of Petrology 28*: 531–567.

Graham, I. J.; Worthington, T. J. 1988: Petrogenesis of Tauhara Dacite (Taupo Volcanic Zone, New Zealand)—evidence for magma mixing between high-alumina andesite and rhyolite. *Journal of Volcanology and Geothermal Research 35*: 279–294.

Graham, I. J.; Gulson, B. L.; Hedenquist, J. W.; Mizon, K. 1992: Petrogenesis of late Cenozoic volcanic rocks from the Taupo Volcanic Zone, New Zealand, in the light of new lead isotope data. *Geochimica et Cosmochimica Acta 56*: 2797–2819.

Graham, I. J.; Cole, J. W.; Briggs, R. M.; Gamble, J. A.; Smith, I. E. M. 1995: Petrology and petrogenesis of volcanic rocks from the Taupo Volcanic Zone: a review. *Journal of Volcanology and Geothermal Research 68*: 59–87.

Hamilton, W. M. 1937: The Little Barrier Island, Hauturu. *New Zealand Department of Scientific and Industrial Research Bulletin 54.*

Hayward, B. W. 1993: The tempestuous 10 million year life of a double arc and intra-arc basin—New Zealand's Northland Basin in the early Miocene. *In*: Ballance, P. F. *ed*. Sedimentary basins of the world, 2: South Pacific sedimentary basins. Amsterdam, Elsevier. Pp. 113–142.

Herzer, R. H.; Mascle, J. 1996: Anatomy of a continent-backarc transform—the Vening Meinesz Fracture Zone northwest of New Zealand. *Marine Geophysical Researches 18*: 401–427.

Hibbard, M. J. 1981: The magma mixing origin of mantled feldspars. *Contributions to Mineralogy and Petrology 76*: 158–170.

Hochstein, M. P.; Ballance, P. F. 1993: Hauraki Rift: a young, active, intra-continental rift in a back-arc setting. *In*: Ballance, P. F. *ed*. Sedimentary basins of the world, 2: South Pacific sedimentary basins. Amsterdam, Elsevier. Pp. 295–305.

Hopgood, A. M.; Barron, R. H. 1954: Notes on the geology of Little Barrier Island. *Tane 6*: 7–19.

Huang, Y.; Hawkesworth, C. J.; van Calsteren, P.; Smith, I. E. M.; Black, P. M. 1997: Melt generation models for the Auckland Volcanic Field, New Zealand: constraints from U-Th isotopes. *Earth and Planetary Science Letters 149*: 67–84.

Isaac, M. J.; Herzer, R. H.; Brook, F. J.; Hayward, B. W. 1994: Cretaceous and Cenozoic sedimentary basins of Northland, New Zealand. *Institute of Geological & Nuclear Sciences Monograph 8.*

Itaya, T.; Nagao, K.; Honjou, Y.; Okada, T.; Ogata, A. 1991: Argon isotope analysis by a newly developed mass spectrometric system for K-Ar dating. *Mineralogical Journal 15*: 203–221.

Kear, D. 1961: Geology. *In*: Hamilton, W. M. *ed*. Little Barrier Island (Hauturu). *New Zealand Department of Scientific and Industrial Research Bulletin 137.* 198 p.

Kretz, R. 1982: Transfer and heat exchange equilibria in a portion of the pyroxene quadrilateral as deduced from natural and experimental data. *Geochimica et Cosmochimica Acta 46*: 411–421.

Kuschel, E.; Smith, I. E. M. 1992: Rare earth mobility in young arc-type volcanic rocks from northern New Zealand. *Geochimica et Cosmochimica Acta 56*: 3951–3955.

Lindsay, J. M. 1995: Little Barrier Volcano: geology and geochemistry. Unpublished MSc thesis, lodged in the Library, The University of Auckland, Auckland, New Zealand.

Maas, R.; McCulloch, M. T. 1991: The provenance of Archean clastic metasediments in the Narryer Gneiss Complex, Western Australia: trace element geochemistry, Nd isotopes, and U-Pb ages for detrital zircons. *Geochimica et Cosmochimica Acta 55*: 1915–1932.

Morimoto, N.; Fabries, J.; Ferguson, A. K.; Ginzburg, I. V.; Ross, M.; Seifert, F. A.; Zussman, J. 1988: Nomenclature of pyroxenes. *Mineralogical Magazine 52*: 535–550.

Nakamura, N. 1974: Determination of REE, Ba, Fe, Mg, Na and K in carbonaceous and ordinary chondrites. *Geochimica et Cosmochimica Acta 38*: 757–775.

Neall, V. E.; Stewart, R. B.; Smith, I. E. M. 1986: History and petrology of the Taranaki volcanoes. *In*: Smith, I. E. M. *ed*. Late Cenozoic volcanism in New Zealand. *Royal Society of New Zealand Bulletin 23*: 251–263.

O'Hara, M. J.; Mathews, R. E. 1981: Geochemical evolution in an advancing, periodically replenished, periodically tapped, continuously fractionated magma chamber. *Journal of the Geological Society of London 138*: 237–277.

Parker, R. J. 1994a: Major element XRF analysis: methods and HP-86 computer programs. *Department of Geology Report 3*. Auckland, The University of Auckland. 32 p.

Parker, R. J. 1994b: Trace element XRF analysis: methods and HP-86 computer programs. *Department of Geology Report 4*. Auckland, The University of Auckland. 46 p.

Pearce, J. A. 1982: Trace element characteristics of lavas from destructive plate boundaries. *In*: Thorpe, R. S. *ed*. Andesites: orogenic andesites and related rocks. Chichester, Wiley. Pp. 525–548.

Pearce, J. A.; Parkinson, I. J. 1993: Trace element models for mantle melting: application to volcanic arc petrogenesis. *In*: Prichard, H. M.; Alabaster, T.; Harris, N. B. W.; Neary, C. R. *ed*. Magmatic processes and plate tectonics. *Geological Society Special Publication 76*: 373–403.

Pearce, J. A.; Peate, D. W. 1995: Tectonic implications of the composition of volcanic arc magmas. *Annual Review of the Earth and Planetary Sciences 23*: 251–285.

Pearce, J. A.; Harris, N. B. W.; Tindle, A. G. 1984: Trace element discrimination diagrams for the tectonic interpretation of granitic rocks. *Journal of Petrology 25*: 956–983.

Price, R. C.; Gray, C. M.; Wilson, R. E.; Frey, F. A.; Taylor, S. R. 1991: The effects of weathering on rare-earth element, Y and Ba abundances in Tertiary basalts from southeastern Australia. *Chemical Geology 93*: 245–265.

Roden, M. F.; Frey, F. A.; Clague, D. A. 1984: Geochemistry of tholeiitic and alkalic lavas from the Koolau Range, Oahu, Hawaii: implications for Hawaiian volcanism. *Earth and Planetary Science Letters 69*: 141–158.

Rollinson, H. R. 1993: Using geochemical data: evaluation, presentation, interpretation. Singapore, Longman Group. 352 p.

Rutherford, M. J.; Hill, P. M. 1993: Magma ascent rates from amphibole breakdown: an experimental study applied to the 1980–1986 Mount St. Helens eruptions. *Journal of Geophysical Research 98*: 19667–19685.

Smith, I. E. M. 1989: New Zealand intraplate volcanism: North Island. *In*: Johnson, R. W.; Knutson, J.; Taylor, S. R. *ed*. Intraplate volcanism in eastern Australia and New Zealand. Cambridge, Cambridge University Press. Pp. 157–162.

Smith, I. E. M.; Chappell, B. W.; Ward, G. K.; Freeman, R. S. 1977: Peralkaline rhyolites associated with andesitic arcs of the southwest Pacific. *Earth and Planetary Science Letters 37*: 230–236.

Smith, I. E. M.; Okada, T.; Itaya, T.; Black, P. M. 1993: Age relationships and tectonic implications of late Cenozoic basaltic volcanism in Northland, New Zealand. *New Zealand Journal of Geology and Geophysics 36*: 385–393.

Steiger, R. H.; Jager, I. 1977: Subcommission on geochronology: convention on the uses of decay constants in geochronology and cosmochronology. *Earth and Planetary Science Letters 36*: 359–362.

Stimac, J. A.; Pearce, T. H. 1992: Textural evidence of mafic-felsic magma interaction in dacite lavas, Clear Lake, California. *American Mineralogist 77*: 795–809.

Takagi, M. 1995: Miocene–Pliocene arc volcanism of the Hauraki region in North Island, New Zealand. Unpublished MSc thesis, lodged in the Library, Okayama University of Science, Misasa, Japan.

Tatsumi, Y.; Hamilton, D. L.; Nesbitt, R. W. 1986: Chemical characteristics of fluid phase release from a subducted lithosphere and origin of arc magmas: evidence from high-pressure experiments and natural rocks. *Journal of Volcanology and Geothermal Research 29*: 293–309.

von Platen, H. 1965: Experimental anatexis and the genesis of migmatites. *In*: Pitcher, W. S.; Flinn, G. W. *ed*. Controls of metamorphism. Edinburgh, Oliver and Boyd. Pp. 203–218.

Williams, I. S.; Claesson, S. 1987: Isotopic evidence for the Precambrian provenance and Caledonian metamorphism of high grade paragneiss from the Seve Nappes, Scandinavian Caledonides, 2: Ion microprobe zircon U-Th-Pb. *Contributions to Mineralogy and Petrology 97*: 205–217.

Wilson, C. J. N.; Houghton, B. F.; McWilliams, M. O.; Lanphere, M. A.; Weaver, S. D.; Briggs, R. M. 1995: Volcanic and structural evolution of Taupo Volcanic Zone, New Zealand: a review. *Journal of Volcanology and Geothermal Research 68*: 1–28.